GEOLOGY | THE GEOLOGICAL SOCIETY OF AMERICA®

https://doi.org/10.1130/G50973.1

Manuscript received 29 November 2022
Revised manuscript received 4 March 2023
Manuscript accepted 17 March 2023

Published online 19 April 2023

To sink, or not to sink: The thermal and density structure of the modern northern Andean arc constrained by xenolith petrology

Lisa Zieman[1,*], Mauricio Ibañez-Mejia[1], Alan D. Rooney[2], Elias Bloch[3], Natalia Pardo[4], Blair Schoene[5], and Dawid Szymanowski[5]

[1]Department of Geosciences, University of Arizona, Tucson, Arizona 85721, USA
[2]Department of Earth and Planetary Sciences, Yale University, New Haven, Connecticut 06511, USA
[3]Institute of Earth Sciences, University of Lausanne, CH-1015 Lausanne, Switzerland
[4]Departamento de Geociencias, Universidad de Los Andes, 111711 Bogotá, Colombia
[5]Department of Geosciences, Princeton University, Princeton, New Jersey 08544, USA

ABSTRACT

The thermal and compositional structure of arcs influence magmatic differentiation and lower-crustal foundering, two key processes impacting the evolution of the continental crust. Although many studies have proposed time scales of lithospheric recycling based on convective downwelling calculations, these models depend on the composition, density (ρ), and thermal structure of the lower crust and mantle, which are difficult to quantify in active continental arcs. Here, we constrained these properties for the Andean Northern Volcanic Zone using direct petrologic observations from a unique suite of lower-crust and mantle xenoliths from Mercaderes, Colombia. Chemical abrasion–isotope dilution–thermal ionization mass spectrometry (CA-ID-TIMS) U-Pb dates for zircons within the host tuff indicate the xenoliths erupted no earlier than 238 (±19) ka and thus capture a recent snapshot of the arc and subarc mantle. Equilibrium pressure-temperature (*P-T*) estimates for 81 xenoliths define three distinct thermal domains, interpreted as (1) a steep conductive geothermal gradient in the lower arc crust; (2) a convecting mantle wedge; and (3) cooled mantle in proximity to the subducting slab. Our results indicate the presence of an ~10–14-km-thick, high-density lithospheric root that is ~0.1 g/cm³ denser than the underlying mantle. Unlike records from exhumed paleo-arcs, Rayleigh-Taylor instability calculations using our *P-T*-ρ constraints are unrealistically short for the northern Andes. We suggest the presence of partial melts in this hot arc root as a potential source of buoyancy preventing or significantly slowing down foundering.

INTRODUCTION

The thermal structure of active continental margins controls fundamental arc processes such as magma generation (e.g., Davies and Stevenson, 1992), volatile recycling (e.g., Grove et al., 2012), deformation and seismicity (Syracuse et al., 2010), and foundering (aka, "delamination") of density-unstable lower arc crust (e.g., Behn and Kelemen, 2006). The pressure (P), temperature (T), and composition of deep crustal material govern its mineralogy, density (ρ), and viscosity, and thus the likelihood and time scales over which lower crust might become unstable (Jull and Kelemen, 2001). Many studies have hypothesized that the lower crust in thickened continental arcs, where P-T conditions can stabilize garnet clinopyroxenite, or "arclogite," becomes denser than its underlying mantle and founders via Rayleigh-Taylor instabilities (RTIs). Consequently, inferences about the time scales of lower-crustal recycling and its effects on uplift, magmatism, and crustal deformation are often based on this mechanism of removal (Behn et al., 2007; DeCelles et al., 2009; Jagoutz and Behn, 2013; Jull and Kelemen, 2001; Molnar and Garzione, 2007).

Despite the strong dependence of crustal recycling and arc dynamics on arc thermal structure, petrologic information from the roots of modern continental arcs remains scarce. Currently, modern subduction zone thermal regimes are inferred predominantly from geophysical observations and numerical models that consider subducting slab speed, age, geometry, and/or surface heat flow (e.g., Syracuse et al., 2010). Petrologic constraints on the thermal conditions characterizing lower arc crust are limited to ancient arcs and include thermobarometry of xenoliths from the Mesozoic Sierra Nevada arc (Chin et al., 2015; Ducea and Saleeby, 1996; Lee et al., 2006; Rautela et al., 2020) and exhumed paleo-arc sections such as those in Kohistan (Burg et al., 2002; Jagoutz and Schmidt, 2013; Ringuette et al., 1999), Talkeetna (Behn and Kelemen, 2006; Hacker et al., 2008), and Cabo Ortegal (Tilhac et al., 2016). Although these localities have been fundamental for shaping our understanding of lower arc crust petrology, extinct arcs lack important geologic context and coupled in situ geophysical observations of their tectonic setting and physical properties (e.g., crustal thickness, gravity data, seismic velocities, and topography).

Here, we investigated the thermal and compositional structure of the Andean Northern Volcanic Zone (NVZ), a thickened active continental arc, using direct petrologic evidence from lower-crust and mantle xenoliths hosted in a Quaternary eruption. We obtained equilibrium P-T-ρ constraints for 62 new xenoliths, which we then used to directly inform RTI growth calculations. Our data allowed us to test existing models for lower-crustal foundering via convective instability and offer key insights on possible sources of buoyancy that may help to stabilize arclogite roots in continental arcs.

GEOLOGIC BACKGROUND

The NVZ is the northernmost active volcanic segment of the Andes, the world's largest continental subduction system. The NVZ extends from 1°S in Ecuador to 5°N in Colombia (Fig. 1). At 1.5°N, a xenolith locality known as Mercaderes preserves an unparalleled record

Lisa Zieman https://orcid.org/0000-0002-0065-2565
*lzieman@arizona.edu

CITATION: Zieman, L., et al., 2023, To sink, or not to sink: The thermal and density structure of the modern northern Andean arc constrained by xenolith petrology: Geology, v. 51, p. 586–590, https://doi.org/10.1130/G50973.1

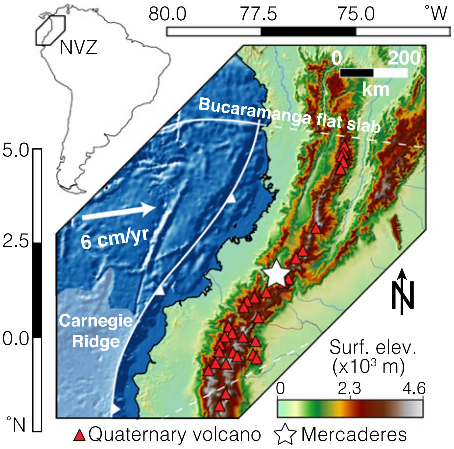

Figure 1. Digital elevation model of the Northern Volcanic Zone (NVZ) in South America and location of Mercaderes, Colombia.

of mafic-ultramafic fragments exhumed by the Granatifera Tuff (GT), a mafic ignimbrite-dominated succession of variably welded lithic-rich tuff breccias and lapilli tuffs deposited from high-concentration pyroclastic density currents.

The Mercaderes xenoliths, described by Weber et al. (2002), Rodriguez-Vargas et al. (2005), and Bloch et al. (2017), include garnet-rich gabbro, hornblendite, pyroxenite, and peridotite fragments. Regional stratigraphic relationships indicate the GT is Quaternary in age, and three garnet clinopyroxenite fragments dated using Lu-Hf have yielded isochrons between 0 and 5.2 Ma (Bloch et al., 2017); however, no previous work has directly dated its eruption.

Based on petrologic, topographic, receiver function, and geoid anomaly observations, Bloch et al. (2017) suggested that a dense arclogite root, sampled by the Mercaderes xenoliths, remains attached to the base of the NVZ crust. Recent seismic data along the Colombian Central Cordillera supports this conclusion; Avellaneda-Jiménez and Monsalve (2022) interpreted a section of lower crust with high shear-wave (Vs) velocity to represent an 8.5–14-km-thick arclogite root at the base of the NVZ.

METHODS AND RESULTS

We obtained zircon U-Pb geochronologic data from two finely laminated ash bed horizons within the mafic GT and an unrelated felsic ignimbrite that unconformably overlies the GT. Zircon grains from the GT ($n = 16$) were dated by chemical abrasion–isotope dilution–thermal ionization mass spectrometry (CA-ID-TIMS) at Princeton University using methods described in the Supplemental Material.[1] Zircon grains from the felsic ignimbrite ($n = 19$) were dated by laser ablation–inductively coupled plasma–mass spectrometry (LA-ICP-MS) at the Arizona LaserChron Center following the methods of Pullen et al. (2018). All U-Pb results are summarized in Tables S1 and S2.

Equilibrium P-T-ρ estimates for 62 garnet-bearing gabbro, pyroxenite, hornblendite, websterite, and peridotite fragments (Fig. 2) were determined using equilibrium thermobarometry between rock-forming phases using multiple calibrations described in detail in the Supplemental Material. Mineral compositions and modal abundances used for these calculations are reported in Table S3, and all thermobarometry results and associated uncertainties are included in Table S4.

ERUPTION AGE OF THE GRANATIFERA TUFF

Zircon from the GT dated via CA-ID-TIMS yielded variable U-Pb dates, ranging from 0.238 ± 0.019 Ma to 65.761 ± 0.054 Ma (Table S1). The youngest zircon provided a maximum eruption age of 238 ± 19 ka. Moderate-precision U-Pb dates from the felsic ignimbrite obtained by LA-ICP-MS also revealed a complex distribution, with dates from 0.282 ± 0.060 Ma to 1.79 ± 0.16 Ma. Because three of the youngest zircon grains from the felsic ignimbrite are within uncertainty of the youngest CA-ID-

[1]Supplemental Material. Analytical methods, thermobarometry and geochronology results, summary of microprobe analyses, and description of instability time scale calculations. Please visit https://doi.org/10.1130/GEOL.S.22306123 to access the supplemental material, and contact editing@geosociety.org with any questions.

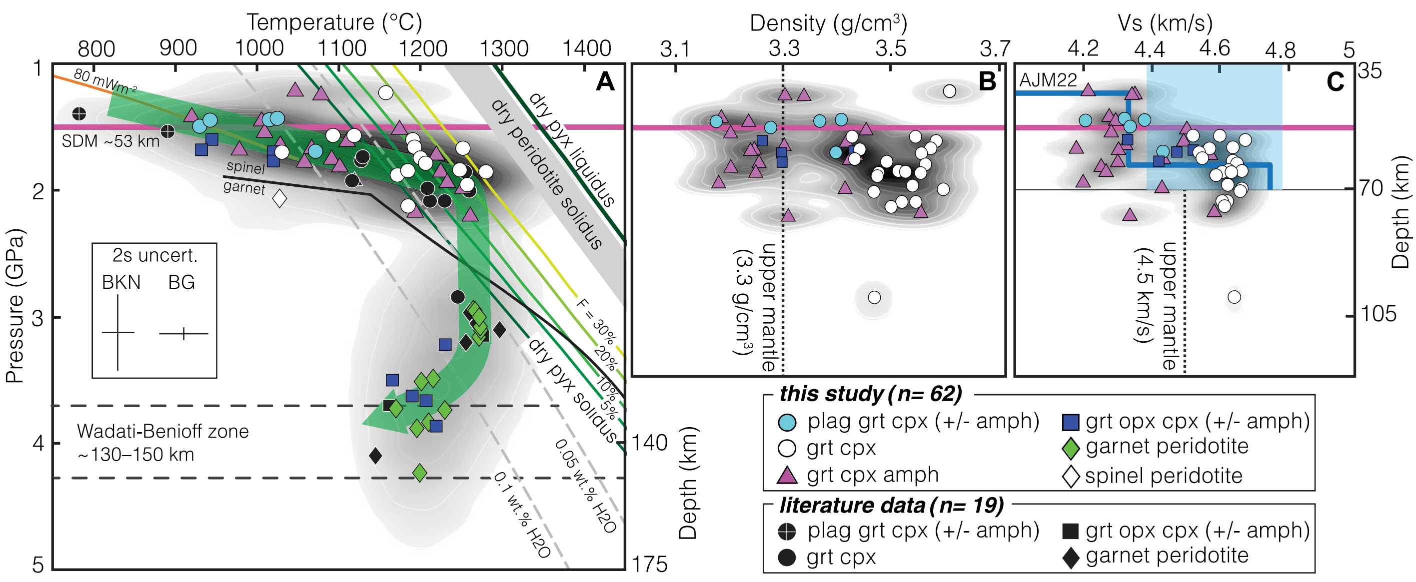

Figure 2. Pressure vs. (A) temperature, (B) density, and (C) shear wave velocity (Vs) for Mercaderes xenoliths. Seismically determined Moho (SDM; pink line) is from Poveda et al. (2015), and Wadati-Benioff zone (dashed black lines) is from Syracuse et al. (2016), using pressure to depth conversion of 35 km/GPa. Solidi are plotted for dry peridotite (gray field; Pertermann and Hirschmann, 2003), hydrous peridotite (dashed gray lines; Katz et al., 2003), and mid-ocean-ridge basalt (MORB)–like garnet clinopyroxenite (green line). Pyroxenite (pyx) dry solidus, liquidus, and melt fraction isopleths (F) are after Pertermann and Hirschmann (2003). Spinel- to garnet-peridotite transition (solid black line) is from Green (1973). Melt-free density (panel B) and Vs (panel C) values for individual xenoliths are compared to upper mantle (pyrolite at 2 GPa, 1250 °C), calculated using methods of Abers and Hacker (2016). Seismic velocity model (AJM22; blue line) is from the proximal Sotará volcano after Avellaneda-Jiménez and Monsalve (2022), as well as their inferred Vs range for arclogite root (blue field). Bivariate probability density contours (light to dark gray shading) were calculated using 2 SD uncertainties of applied thermobarometers (error bars labeled BKN and BG; see Supplemental Material [see text footnote 1] for details) and our estimated modal abundances. Plag—plagioclase; grt—garnet; cpx—clinopyroxene; amph—amphibole; opx—orthopyroxene.

TIMS date from the GT, we consider the latter as the best age estimate for the GT eruption. Our U-Pb results demonstrate that the GT is no older than the mid-Pleistocene, implying that the xenoliths within this tuff capture a geologically recent "snapshot" of the petrologic nature of the NVZ arc.

THERMAL AND PETROLOGIC STRUCTURE OF THE NORTH ANDEAN ARC

The equilibrium *P-T* conditions of Mercaderes xenoliths from this study ($n = 62$) and from previous work ($n = 19$; Bloch et al., 2017; Weber et al., 2002) are shown in Figure 2A. Garnet-bearing gabbro, hornblendite, and clinopyroxenite fragments dominantly equilibrated at 1.2–2.2 GPa and 920–1280 °C, and they define a steep, conductive-like thermal profile interpreted to represent the lower lithosphere. Density and Vs estimates for these lower lithospheric samples, calculated using the methods of Abers and Hacker (2016), suggest this layer is on average denser and seismically faster than the underlying mantle (Figs. 2B–2C). Our new estimates are consistent with recent seismic data (Avellaneda-Jiménez and Monsalve, 2022), which indicate the presence of a > 10-km-thick, high-velocity arclogite root at depths up to 73 km in our study area.

Compared to the global record of arclogite xenoliths and exhumed sections (Ducea et al., 2021), the NVZ arclogites studied here represent a hot end member. The temperatures we obtained are consistent with those expected for deep crustal hot zones (1100–1240 °C; Annen et al., 2006), and many lie above the pyroxenite solidus, suggesting the arclogite root is in a partially molten state. Thus, the hot arc root temperatures in the NVZ and consequential pyroxenite partial melts may influence arc magma geochemistry as well as the style and time scale of lower-crustal foundering (discussed below).

Most mantle-derived garnet peridotite xenoliths ($n = 10$) equilibrated at 2.9–3.2 GPa within a narrow temperature range (1260–1290 °C). This temperature coincides with the hottest arclogites at the base of the lithosphere, thus defining an adiabatic-like thermal profile interpreted as representing the convective thermal regime in the mantle wedge. Another subset of strongly deformed garnet peridotites ($n = 8$) and garnet websterites ($n = 7$) records ~50–100 °C lower temperatures (1140–1230 °C) at higher pressures (3.5–4.1 GPa). The calculated depth of the latter closely approaches, or overlaps within uncertainty, the Wadati-Benioff zone of the subducted Nazca oceanic plate at ~130–150 km beneath Mercaderes (Syracuse et al., 2016), and so this subset is interpreted to reflect cooling of the mantle in proximity to the subducting slab as predicted by thermal models (e.g., Syracuse et al., 2010). All our >3.5 GPa peridotite and websterite fragments showed textural evidence for strong deformation, including undulating extinction in pyroxene and olivine as well as pyroxene porphyroclasts in fine-grained olivine matrices, potentially preserving evidence for strong shearing deformation of the mantle at near-slab depths.

IMPLICATIONS FOR ARCLOGITE FOUNDERING

Studies on lithospheric foundering typically model detachment as RTI, or as viscous downwelling of a negatively buoyant lower-crust layer into the underlying mantle (Behn et al., 2007; Jagoutz and Behn, 2013; Jull and Kelemen, 2001; Molnar and Garzione, 2007). The most important factors controlling the growth rate of a RTI are density and viscosity, which depend on the *P-T* conditions and composition/mineralogy of the crust and mantle. Whereas these parameters have to be either assumed or inferred through geophysics in most cases, our xenolith results directly constrain these parameters for the NVZ, so RTI calculations specific to this region can be performed.

Using density calculations for our samples (Fig. 2B), the bulk density contrast ($\Delta\rho$) of a melt-free NVZ crustal root relative to peridotite at similar *P-T* conditions is ~0.1 g/cm³, confirming that solids in the NVZ arc root are negatively buoyant with respect to the underlying mantle. Instability time scales for the NVZ were calculated after Jull and Kelemen (2001) and Behn et al. (2007) and were compared to published RTI time scales for the Kohistan and Talkeetna arcs (Fig. 3A). To allow comparison with the Kohistan and Talkeetna models, our calculations used the same RTI model parameters described for these paleo-arcs by Jagoutz and Behn (2013), with the exception of T and $\Delta\rho$, because these parameters were directly constrained by our data. The NVZ arc root is predicted to founder via RTI on exceedingly short time scales given the hotter temperature at the base of the NVZ lithosphere. Our modeling indicates the NVZ instability growth time is far shorter than the time required for the arc root to grow, given reasonable magma supply rates, and the root thickness should not exceed ~1 km before detaching. However, an ~10–14-km-thick arclogite root is clearly present, as evidenced by our xenoliths and seismic data (Avellaneda-Jiménez and Monsalve, 2022).

The discrepancy between the RTI model and observed arc root thickness in the NVZ could be reconciled if an additional source of buoyancy could keep the root stabilized over time scales exceeding those expected from these calculations. The density estimates for our samples using the methods of Abers and Hacker (2016) assume a melt-free root (Fig. 2B); however, many garnet pyroxenite fragments equilibrated at conditions above the pyroxenite solidus (Fig. 2A), implying partial melts are expected to be present in this deep crustal hot zone. Bowman et al. (2021) demonstrated that low quantities of trapped melt in an arclogite root can decrease viscosity and cause rapid foundering, but greater melt fractions can have the opposite effect, increasing the overall buoyancy of the root and stabilizing it over longer time scales. Given that the NVZ arclogites are a hot end member of global arclogites (Ducea et al., 2021), our study area provides an ideal locality in which to evaluate the hypothesis that melt-

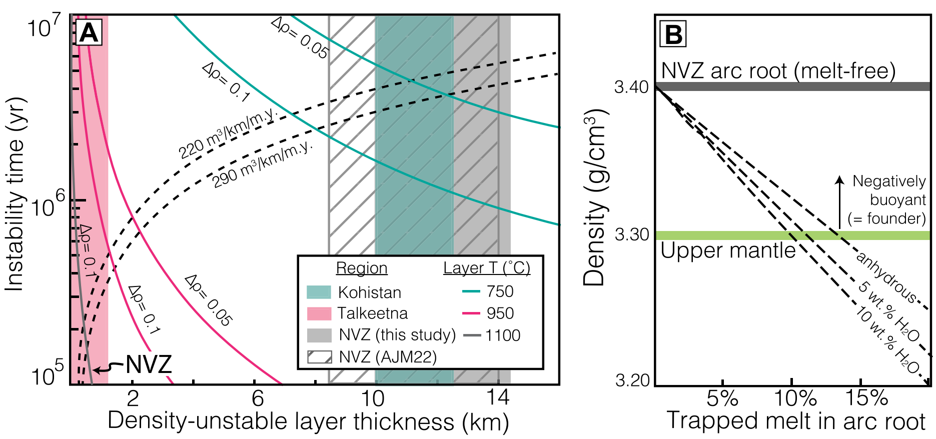

Figure 3. Rayleigh-Taylor instability time vs. density-unstable layer thickness calculated after Jull and Kelemen (2001) and Behn et al. (2007). (A) Instability time curves for density contrasts ($\Delta\rho$) of 0.05 and 0.1 g/cm³ and layer temperatures for Kohistan (750 °C; Ringuette et al., 1999), Talkeetna (950 °C; Hacker et al., 2008), and Mercaderes (1100 °C; midlayer temperature in Fig. 2A). Thickness of the Northern Volcanic Zone (NVZ) root (10–14 km) is constrained by thermobarometry and geophysics. Cumulate layer thickness growth rates (dashed lines) assume 70% crystallization from typical arc magma fluxes to form cumulate layer (Jagoutz and Schmidt, 2013). (B) Density vs. trapped melt within arc root showing effects on bulk root density caused by adding variable amounts of anhydrous (ρ = 2.65 g/cm³) and hydrous (5 and 10 wt% H_2O; ρ = 2.5 g/cm³ and 2.4 g/cm³, respectively) intermediate melt, using melt densities from Malfait et al. (2014) at 2 GPa and 1100 °C.

assisted buoyancy can stabilize high-density roots beyond the temporal bounds imposed by melt-free RTI calculations.

In Figure 3B, the bulk density of the NVZ arc root was calculated as a function of melt fraction present. The decrease in bulk root density caused by the addition of an ~10% fraction of hydrous (10 wt% H_2O) partial melt is sufficient to completely stabilize it (i.e., make the root density equal to that of peridotite; Fig. 3B). Although estimates for melt segregation and percolation in partially molten arclogites are lacking, studies in granitic systems suggest that melt fractions between 8% and 20% will allow melt to connect locally (over centimeters to decimeters) but not allow it to escape over larger distances (Vigneresse et al., 1996). Therefore, ~10% is a reasonable partial melt fraction that will sufficiently decrease bulk density but only locally interconnect within the arc root and not be extracted. Furthermore, the melt-free Vs estimates we calculated for the arclogite samples (Fig. 2C) are broadly consistent with the velocity structure observed by Avellaneda-Jiménez and Monsalve (2022), while the uncertainty on the absolute velocity of their seismic model may allow for the presence of melt. We propose that the hot thermal regime of the NVZ arc enables the presence of sufficient buoyant partial melts to prevent the arc root from rapidly foundering as a melt-free RTI, contrasting with observations from "cooler" arc settings, including the Central Andes, the Sierra Nevada, and the Talkeetna and Kohistan paleo-arcs.

ACKNOWLEDGMENTS

We thank Mark Behn for kindly providing code and insights for Rayleigh-Taylor instability modeling. We acknowledge support from National Science Foundation (NSF) grants EAR-2131643 (to M. Ibañez-Mejia) and EAR-1926421 (to A. Rooney). L. Zieman thanks the Awards for Geochronology Student Research program for support (NSF grants EAR-1759200 and EAR-1759353). We thank Urs Schaltegger for editorial handling and reviewers Catherine Annen, Mark Behn, and Michel Gregoire for their constructive feedback.

REFERENCES CITED

Abers, G.A., and Hacker, B.R., 2016, A MATLAB toolbox and Excel workbook for calculating the densities, seismic wave speeds, and major element composition of minerals and rocks at pressure and temperature: Geochemistry Geophysics Geosystems, v. 17, no. 2, p. 616–624, https://doi.org/10.1002/2015GC006171.

Annen, C., Blundy, J.D., and Sparks, R.S.J., 2006, The genesis of intermediate and silicic magmas in deep crustal hot zones: Journal of Petrology, v. 47, no. 3, p. 505–539, https://doi.org/10.1093/petrology/egi084.

Avellaneda-Jiménez, D.S., and Monsalve, G., 2022, Arclogite nature of the Colombian Andes magmatic arc root: A receiver-function approach: Tectonophysics, v. 836, https://doi.org/10.1016/j.tecto.2022.229417.

Behn, M.D., and Kelemen, P.B., 2006, Stability of arc lower crust: Insights from the Talkeetna arc section, south central Alaska, and the seismic structure of modern arcs: Journal of Geophysical Research–Solid Earth, v. 111, no. B11, https://doi.org/10.1029/2006JB004327.

Behn, M.D., Hirth, G., and Kelemen, P.B., 2007, Trench-parallel anisotropy produced by foundering of arc lower crust: Science, v. 317, no. 5834, p. 108–111, https://doi.org/10.1126/science.1141269.

Bloch, E., Ibañez-Mejia, M., Murray, K., Vervoort, J., and Müntener, O., 2017, Recent crustal foundering in the Northern volcanic zone of the Andean arc: Petrological insights from the roots of a modern subduction zone: Earth and Planetary Science Letters, v. 476, p. 47–58, https://doi.org/10.1016/j.epsl.2017.07.041.

Bowman, E.E., Ducea, M.N., and Triantafyllou, A., 2021, Arclogites in the subarc lower crust: Effects of crystallization, partial melting, and retained melt on the foundering ability of residual roots: Journal of Petrology, v. 62, no. 12, https://doi.org/10.1093/petrology/egab094.

Burg, J.-P., Bodinier, J.-L., Chaudhry, S., Hussain, S., and Dawood, H., 2002, Infra-arc mantle-crust transition and intra-arc mantle diapirs in the Kohistan Complex (Pakistani Himalaya): Petro-structural evidence: Terra Nova, v. 10, no. 2, p. 74–80, https://doi.org/10.1046/j.1365-3121.1998.00170.x.

Chin, E.J., Lee, C.T.A., and Blichert-Toft, J., 2015, Growth of upper plate lithosphere controls tempo of arc magmatism: Constraints from Al-diffusion kinetics and coupled Lu-Hf and Sm-Nd chronology: Geochemical Perspectives Letters, v. 1, no. 1, p. 20–32, https://doi.org/10.7185/geochemlet.1503.

Davies, J.H., and Stevenson, D.J., 1992, Physical model of source region of subduction zone volcanics: Journal of Geophysical Research, v. 97, p. 2037–2070, https://doi.org/10.1029/91JB02571.

DeCelles, P.G., Ducea, M.N., Kapp, P., and Zandt, G., 2009, Cyclicity in Cordilleran orogenic systems: Nature Geoscience, v. 2, no. 4, p. 251–257, https://doi.org/10.1038/ngeo469.

Ducea, M.N., and Saleeby, J.B., 1996, Buoyancy sources for a large, unrooted mountain range, the Sierra Nevada, California: Evidence from xenolith thermobarometry: Journal of Geophysical Research–Solid Earth, v. 101, no. B4, p. 8229–8244, https://doi.org/10.1029/95JB03452.

Ducea, M.N., Chapman, A.D., Bowman, E., and Triantafyllou, A., 2021, Arclogites and their role in continental evolution. Part 1: Background, locations, petrography, geochemistry, chronology and thermobarometry: Earth-Science Reviews, v. 214, https://doi.org/10.1016/j.earscirev.2020.103375.

Green, D.H., 1973, Experimental melting studies on a model upper mantle composition at high pressure under water-saturated conditions: Earth and Planetary Science Letters, v. 19, p. 37–53, https://doi.org/10.1016/0012-821X(73)90176-3.

Grove, T.L., Till, C.B., and Krawczynski, M.J., 2012, The role of H_2O in subduction zone magmatism: Annual Review of Earth and Planetary Sciences, v. 40, no. 1, p. 413–439, https://doi.org/10.1146/annurev-earth-042711-105310.

Hacker, B.R., Mehl, L., Kelemen, P.B., Rioux, M., Behn, M.D., and Luffi, P., 2008, Reconstruction of the Talkeetna intraoceanic arc of Alaska through thermobarometry: Journal of Geophysical Research, v. 113, no. B3, https://doi.org/10.1029/2007JB005208.

Jagoutz, O., and Behn, M.D., 2013, Foundering of lower island-arc crust as an explanation for the origin of the continental Moho: Nature, v. 504, p. 131–134, https://doi.org/10.1038/nature12758.

Jagoutz, O., and Schmidt, M.W., 2013, The composition of the foundered complement to the continental crust and a re-evaluation of fluxes in arcs: Earth and Planetary Science Letters, v. 371–372, p. 177–190, https://doi.org/10.1016/j.epsl.2013.03.051.

Jull, M., and Kelemen, P.B., 2001, On the conditions for lower crustal convective instability: Journal of Geophysical Research–Solid Earth, v. 106, no. B4, p. 6423–6446, https://doi.org/10.1029/2000JB900357.

Katz, R.F., Spiegelman, M., and Langmuir, C.H., 2003, A new parameterization of hydrous mantle melting: Geochemistry Geophysics Geosystems, v. 4, no. 9, https://doi.org/10.1029/2002GC000433.

Lee, C.-T.A., Cheng, X., and Horodyskyj, U., 2006, The development and refinement of continental arcs by primary basaltic magmatism, garnet pyroxenite accumulation, basaltic recharge and delamination: Insights from the Sierra Nevada, California: Contributions to Mineralogy and Petrology, v. 151, no. 2, p. 222–242, https://doi.org/10.1007/s00410-005-0056-1.

Malfait, W.J., Seifert, R., Petitgirard, S., Mezouar, M., and Sanchez-Valle, C., 2014, The density of andesitic melts and the compressibility of dissolved water in silicate melts at crustal and upper mantle conditions: Earth and Planetary Science Letters, v. 393, p. 31–38, https://doi.org/10.1016/j.epsl.2014.02.042.

Molnar, P., and Garzione, C.N., 2007, Bounds on the viscosity coefficient of continental lithosphere from removal of mantle lithosphere beneath the Altiplano and Eastern Cordillera: Tectonics, v. 26, no. 2, TC2013, https://doi.org/10.1029/2006TC001964.

Pertermann, M., and Hirschmann, M.M., 2003, Partial melting experiments on a MORB-like pyroxenite between 2 and 3 GPa: Constraints on the presence of pyroxenite in basalt source regions from solidus location and melting rate: Journal of Geophysical Research–Solid Earth, v. 108, no. B2, 2125, https://doi.org/10.1029/2000JB000118.

Poveda, E., Monsalve, G., and Vargas, C.A., 2015, Receiver functions and crustal structure of the northwestern Andean region, Colombia: Journal of Geophysical Research–Solid Earth, v. 120, no. 4, p. 2408–2425, https://doi.org/10.1002/2014JB011304.

Pullen, A., Ibáñez-Mejia, M., Gehrels, G.E., Giesler, D., and Pecha, M., 2018, Optimization of a laser ablation–single collector–inductively coupled plasma–mass spectrometer (Thermo Element 2) for accurate, precise, and efficient zircon U-Th-Pb geochronology: Geochemistry Geophysics Geosystems, v. 19, no. 10, p. 3689–3705, https://doi.org/10.1029/2018GC007889.

Rautela, O., Chapman, A.D., Shields, J.E., Ducea, M.N., Lee, C.-T., Jiang, H., and Saleeby, J., 2020, In search for the missing arc root of the Southern California Batholith: *P-T-t* evolution of upper mantle xenoliths of the Colorado Plateau transition zone: Earth and Planetary Science Letters, v. 547, https://doi.org/10.1016/j.epsl.2020.116447.

Ringuette, L., Martignole, J., and Windley, B.F., 1999, Magmatic crystallization, isobaric cooling, and decompression of the garnet-bearing assemblages of the Jijal sequence (Kohistan terrane, western Himalayas): Geology, v. 27, no. 2, p. 139–142, https://doi.org/10.1130/0091-7613(1999)027<0139:MCICAD>2.3.CO;2.

Rodriguez-Vargas, A., Koester, E., Mallmann, G., Conceição, R.V., Kawashita, K., and Weber, M.B.I., 2005, Mantle diversity beneath the Colombian Andes, Northern volcanic zone: Constraints from Sr and Nd isotopes: Lithos, v. 82, no. 3–4, p. 471–484, https://doi.org/10.1016/j.lithos.2004.09.027.

Syracuse, E.M., van Keken, P.E., and Abers, G.A., 2010, The global range of subduction zone thermal models: Physics of the Earth and Planetary Interiors, v. 183, no. 1–2, p. 73–90, https://doi.org/10.1016/j.pepi.2010.02.004.

Syracuse, E.M., Maceira, M., Prieto, G.A., Zhang, H., and Ammon, C.J., 2016, Multiple plates subducting beneath Colombia, as illuminated by seismicity and velocity from the joint inversion of seismic and gravity data: Earth and Planetary Science Letters, v. 444, p. 139–149, https://doi.org/10.1016/j.epsl.2016.03.050.

Tilhac, R., Ceuleneer, G., Griffin, W.L., O'Reilly, S.Y., Pearson, N.J., Benoit, M., Henry, H., Girardeau, J., and Gregoire, M., 2016, Primitive arc magmatism and delamination: Petrology and geochemistry of pyroxenites from the Cabo Ortegal complex, Spain: Journal of Petrology, v. 57, no. 10, p. 1921–1954, https://doi.org/10.1093/petrology/egw064.

Vigneresse, J.L., Barbey, P., and Cuney, M., 1996, Rheological transitions during partial melting and crystallization with application to felsic magma segregation and transfer: Journal of Petrology, v. 37, no. 6, p. 1579–1600, https://doi.org/10.1093/petrology/37.6.1579.

Weber, M.B.I., Tarney, J., Kempton, P.D., and Kent, R.W., 2002, Crustal make-up of the North Andes: Evidence based on deep crustal xenolith suites, Mercaderes, SW Colombia: Tectonophysics, v. 345, p. 49–82, https://doi.org/10.1016/S0040-1951(01)00206-2.

Printed in USA